Progress In Electromagnetics Research Letters, Vol. 103, 99–107, 2022

Design of a Highly Sensitive Sensor for Measuring Liquid Permittivity with Flexible Substrate

Bo Yin, Xiangyu Shi*, Juntao Yin, and Junguang Chen

Abstract—To further improve the sensitivity of liquid dielectric constant measurements, a cylindrical container-type dielectric constant sensor is proposed in this paper. The container of the sensor consists of a substrate integrated waveguide (SIW) loaded with complementary split ring resonators (CSRRs) and a microstrip line. In order to solve the problem that the electric field distribution of the traditional container liquid dielectric constant sensor is only in a single plane, which cannot obtain good resonance characteristics, the sidewall of the sensor container is surrounded by a flexible material loaded with CSRR-SIW. Higher sensitivity can be obtained from measuring dielectric constant with more concentrated electric field distribution. The simulation results show that when the permittivity of the liquid under test (LUT) changes from 1 to 10, the resonance frequency of the sensor changes from 4.50 GHz to 2.94 GHz. The resonance frequency shift with unit dielectric constant greater than 150 MHz is realized. Using the relationship between the fitting permittivity and resonance frequency, the measurement of the known liquid permittivity of the standard sample is carried out. The test results show that the relative error is less than 2%, and the test sensitivity is 3.85%.

1. INTRODUCTION

The dielectric constant is a macroscopic parameter describing dielectric material, which plays an important role in production and scientific research [1, 2]. Accurate measurement of dielectric constant of liquid materials can indirectly characterize the biological properties of the system. In biology [3], nondestructive testing of biological samples is realized. In medical treatment[4], doctors can judge the early pathology by detecting the tissue water content before and after the lesion, and make an early pathological judgment. In industrial production [5], the concentration of chemical mixed organic liquid can be detected.

Common methods for measuring dielectric constant of liquid include waveguide method [6], free space method [7], and resonant cavity method [8]. Among them, resonant cavity method has become the main method to measure the dielectric constant of liquid for its high sensitivity, high precision, and low cost. The method of measuring the permittivity of liquid by microwave method can be divided into plane type [9, 10], container type [11, 12], and intrusive type [13, 14]. In recent years, many studies on the measurement of liquid dielectric constant have been reported. A helical coupled passive resonator is proposed by Koirala et al. [9], which uses a micropipette to drop the measured liquid onto the sensor surface. The planar liquid dielectric sensor needs to accurately control the volume of the liquid. By dropping the LUT on the surface of the sensor, the dielectric constant of the LUT can be measured by obtaining the resonance frequency offset. This method is simple in design and measurement, but it cannot accurately control the volume of the liquid to be measured, and it is easy to seep and corrode the sensor. Based on the planar liquid sensor, the container of liquid storage is added. Abdolrazzaghi

Received 12 January 2022, Accepted 29 March 2022, Scheduled 30 March 2022
* Corresponding author: Xiangyu Shi (641151299@qq.com).
The authors are with the School of Optoelectronic Engineering, Chongqing University of Posts and Telecommunications, Chongqing 400065, China.

put the LUT stored in a plastic tube on a metamaterial resonator to measure the dielectric constant of the liquid [11]. Similarly, in [12] the LUT is placed on a plastic tube of the dielectric substrate to measure the dielectric constant [12]. The container can better store the LUT and solve the problem of liquid leakage of the sensor. However, the electric field is only concentrated in a single plane which cannot fully contact with the liquid to be measured, so the sensitivity of the sensor is not high enough. For the intrusion type detection method, a novel design of intrusive type sensor is proposed for liquid adulteration detection by Nilesh et al. [13]. Two CSRRs were etched on the proposed horn structure to form a compact design with improved sensitivity in this work. Reyes-Vera proposed an intrusive liquid dielectric constant sensor [14], which was used as a probe to be placed into the LUT. In this way, the liquid to be tested can be in full contact with the sensor. But the volume of the liquid to be measured needs to be larger than that of the sensor, and the sensor will pollute the liquid to be measured itself. Three types of liquid dielectric constant detection methods have their advantages and disadvantages. The key to ameliorating the performance of the dielectric constant measurement based on the resonant cavity method is to optimize the distribution of the electric field in the measuring area.

In order to solve the problems of the liquid microwave sensor mentioned above, a liquid dielectric constant microwave sensor with a cylindrical container structure is proposed in this paper. The sensor consists of two parts. The bottom is the substrate loaded with CSRR medium. The top is a cylinder surrounded by flexible materials, and the inside wall is loaded with CSRR-SIW. Compared with the traditional liquid sensor, the container surrounded by a flexible SIW-CSRR greatly improves the electric field intensity distribution in the liquid area to be measured. The widespread distributed electric field strength makes the sensor more sensitive to the change of dielectric constant, which further improves the sensitivity of dielectric constant detection.

2. ANALYSIS OF THEORY

SIW is a waveguide structure with low insertion loss and low radiation, which can be integrated on a dielectric substrate [15]. The top and bottom of the SIW are metal patches with periodically arranged metallized vias on either side. Compared with traditional metal waveguides, SIW not only inherits the advantages of low loss and high quality factor of traditional waveguides but also has the advantages of low cost and easy planar integration, which is more suitable for the application of miniaturized microwave and millimetre wave circuits. Metallized vias on both sides of the dielectric substrate can be equivalent to the two side walls of the traditional metal waveguide, whose function is to limit the propagation of electromagnetic fields in SIW. Its structure is shown in Figure 1(a). To eliminate the influence of metallized vias on electromagnetic wave leakage on the SIW as much as possible, the structural parameters of SIW need to satisfy the following relationship [16]:

$$d < 0.2\lambda_g, \quad p < 2d, \quad d < 0.4w_0$$

The conventional metal waveguide has the following conversion relationship with SIW:

$$w_{eff} = w_0 - 1.08 \times \frac{d^2}{0.95p}$$

where w_0 and w_{eff} represent the actual physical width and equivalent width of SIW, respectively.

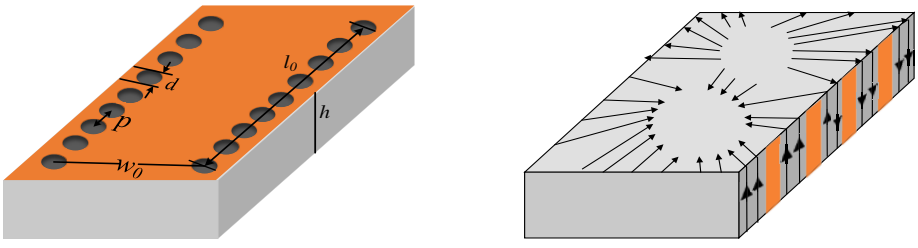

Figure 1. The structure of SIW. (a) 3-D view; (b) current distribution of SIW.

Because the metallized vias are added to the dielectric substrate, it is equivalent to adding a gap to the narrow wall of the rectangular waveguide. Therefore, when the electromagnetic wave propagates in the direction perpendicular to the gap, the current line will be cut off by the metallized vias, which will generate strong radiation. When the electromagnetic wave of TE_{m0} mode propagates in SIW, the propagation direction of the electromagnetic wave is parallel to the metallized vias, so the current line will not be cut off by the metal array metallized vias; SIW can only transmit TE mode and only excite and transmit TE_{m0} mode. When the main mode TE_{10} propagates inside SIW, the distribution of its surface current is as shown in Figure 1(b).

CSRR is the dual structure of SRR, which improves the sensitivity of microwave circuit to frequency offset by etching a gap in the shape of an open resonant ring in the metal plane. Its structure and equivalent circuit are shown in Figure 2. The excitation of CSRR mainly comes from the electric field perpendicular to the ring plane and the magnetic field parallel to the ring plane, and the electric field excitation is obviously higher than the magnetic field excitation. When CSRR works near the resonant frequency, it can be equivalent to an electric dipole, which will produce a negative dielectric constant near the resonant frequency, with band-stop effect [17].

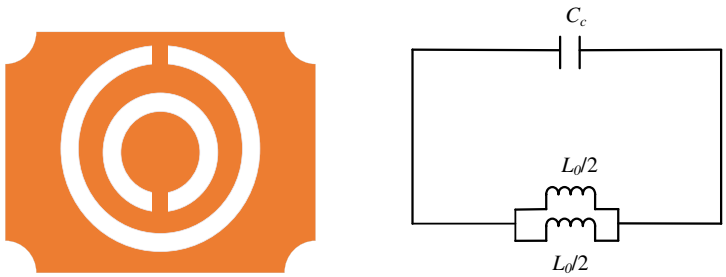

Figure 2. (a) The structure of CSRR; (b) the equivalent circuit.

The inductor L_c can be equivalent to two-loop inductors of CSRR in parallel. The metal ring between the slots and the underlying ground metal can be coupled to form the capacitor C_c. When the CSRR structure is excited by the electromagnetic wave normal to the surface, CSRR can be regarded as an LC resonant circuit. The resonant frequency of the CSRR is determined by

$$f = \frac{1}{2\pi\sqrt{L_c C_c}}$$

When CSRR operates near the resonant frequency, it can be equivalent to an electric dipole. There is a negative dielectric constant near the resonance frequency, which has a band-stop effect and a resonance absorption peak.

3. STRUCTURAL DESIGN

The cylinder container sensor for liquid dielectric constant detection proposed in this paper is shown in Figure 3. The structure of the sensor consists of a cylinder sidewall and a bottom substrate. The 3-D view of the sensor is shown in Figure 3(a). The sidewall of the container is a cylindrical structure surrounded by a flexible material polyimide with a thickness of 0.170 mm, which is loaded with a CSRR-SIW. The substrate loaded with a CSRR-SIW forms a metal-dielectric-metal three-layer structure through metallized vias. To better present the structural integrity of the sensor, Figure 3(b) shows the exploded view at 50% transparency. The inner and outer sides of the flexible substrate are shown in Figure 3(c) and Figure 3(d), respectively. The bottom layer of the container is a CSRR loaded microstrip structure. The bottom medium of the sensor is Rogers 5880 with a thickness of 0.787 mm, as shown in Figure 3(e) and Figure 3(f). Microstrip and CSRR are loaded on the upper surface, and the lower surface is coated with copper. The volume of the container is about 2.0 ml, and a plastic film with a thickness of 0.008 mm is arranged between the liquid and the inside wall of the container. The

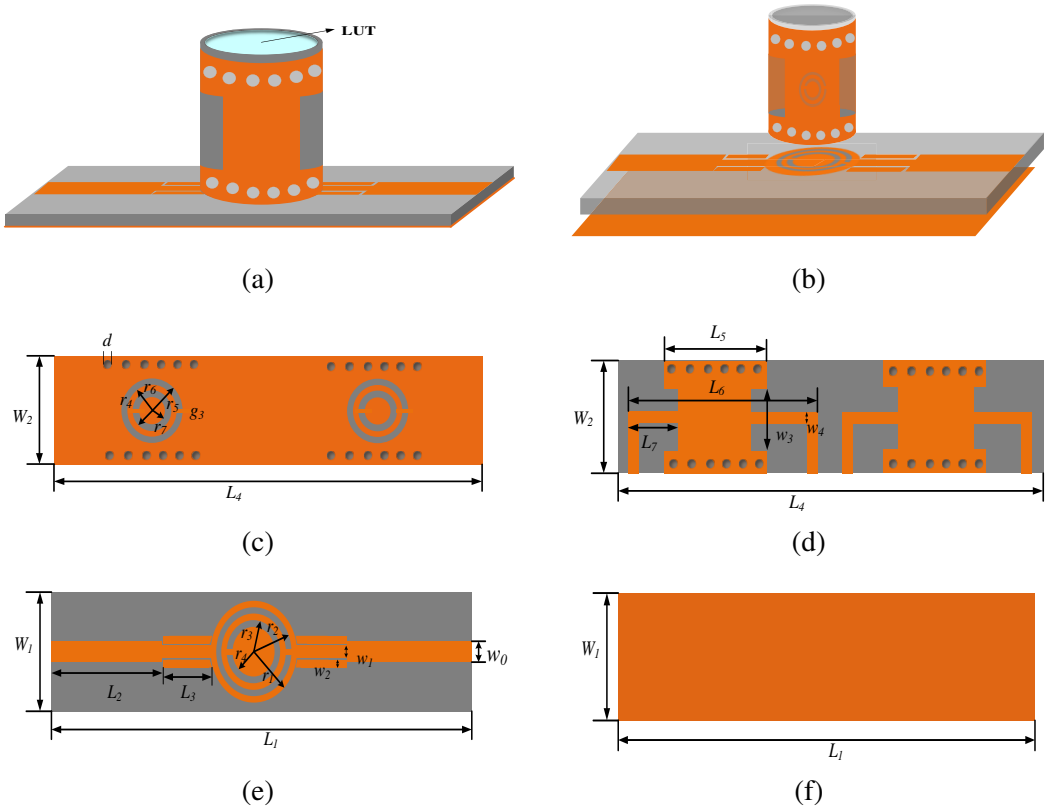

Figure 3. Sensor structure. (a) 3-D view; (b) 50% transparency exploded view; (c) expansion view of container inner wall; (d) expansion view of container outer wall; (e) top view of substrate; (f) bottom view of substrate.

electric field in the plane of the container is transferred to the inside of the side surface through SIW and directly acts on the liquid to be measured through CSRR, which greatly strengthens the electric field intensity of the area to be measured and enhances the sensitivity of the sensor. The specific parameters of the sensor are shown in Table 1.

Table 1. The design parameter value.

Parameter	Size (mm)	Parameter	Size (mm)	Parameter	Size (mm)	Parameter	Size (mm)
L_1	60.0	w_2	0.9	W_2	12.0	w_4	0.9
W_1	10.0	r_1	5.2	L_5	12.0	g	0.4
L_2	14.0	r_2	4.8	L_6	21.3	r_5	3.0
L_3	8.8	r_3	4.2	L_7	6.0	r_6	2.6
w_0	2.4	r_4	3.8	d	1.0	r_7	2.2
w_1	1.0	L_4	45.2	w_3	6.0	r_8	1.8

In order to design and optimize the size of the sensor and obtain the relationship between the resonant frequency and dielectric constant, three-dimensional electromagnetic simulation software ANSYS HFSS is used in this paper. The simulation results show that when the dielectric constant of the liquid to be measured changes from 1 to 10, the resonant frequency of the sensor changes from 4.50 GHz to 2.94 GHz, and the frequency offset is 1.56 GHz. The calculated reflection coefficient S_{11}, corresponding to each MUT is plotted together with the change of dielectric constant, as shown in

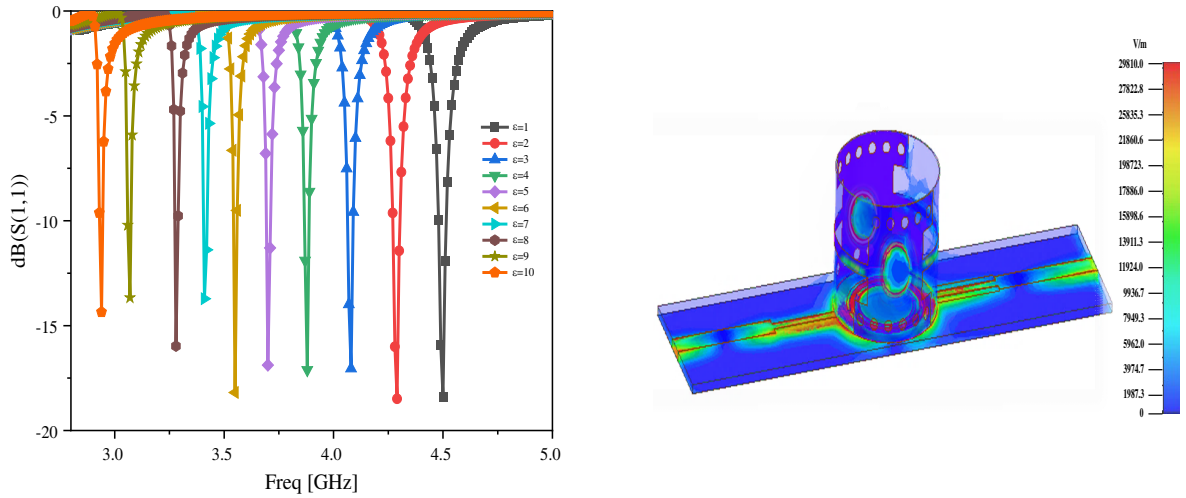

Figure 4. Simulation results. (a) Reflection coefficients under various dielectric constant of LUTs, $\varepsilon = 1$–10; (b) the electric field distribution of the sensor.

Figure 4(a). Figure 4(b) shows the electric field distribution of the sensor without the LUT. The highest intensity reaches 2.981×10^4 V/m.

According to the data in Figure 4(a), the digital relationship between the relative dielectric constant and resonant frequency can be fitted. The fitting curve is shown in Figure 5. The goodness of fit $R^2 = 0.998$. The mathematical model for the sensor is expressed as:

$$\varepsilon = 0.8253f^2 - 11.9577f + 38.0697$$

In order to further study the influence on dielectric constant sensitivity from the designed cylinder structure, we simulated the LUT placed in a plastic container. According to the simulation results shown in Figure 6, the resonant frequency of the sensor corresponding to the glass container is shifted from 5.84 GHz to 6.82 GHz, shifted by 980 MHz. Compared with the designed sensor, the frequency offset is significantly reduced, and the bandwidth is also widened.

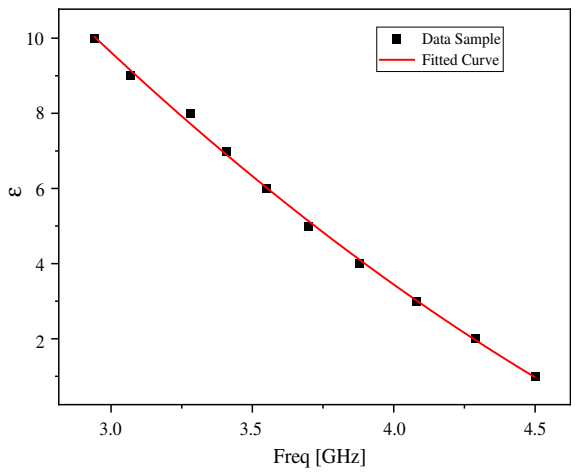

Figure 5. Simulation results. Polynomial fitting of frequency and dielectric constant.

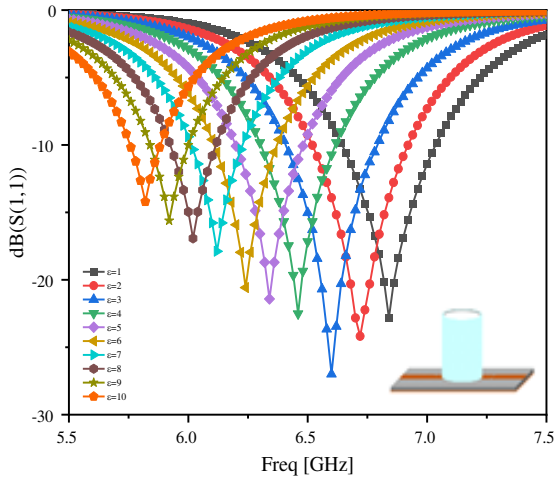

Figure 6. Simulated reflection coefficients under various dielectric constants in the glass container of the LUTs, $\varepsilon = 1$–10.

4. EXPERIMENT AND DISCUSSION

To demonstrate the design, the proposed sensor is fabricated and measured, which is presented in Figure 7. The flexible substrate bends to form the sidewall of the cylindrical container and is connected to the bottom dielectric substrate by a welding process.

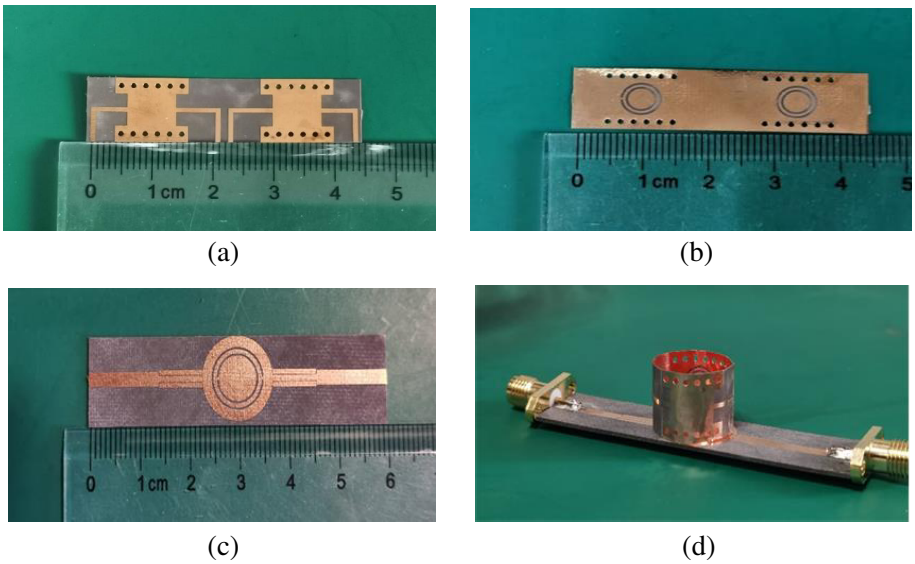

Figure 7. Material objects. (a) Top of flexible substrate; (b) bottom of flexible substrate; (c) bottom substrate; (d) the fabricated sensor.

The processed substrate is connected with an SMA connector and Agilent N5242A PNA-X Vector network. Experimental environment construction and samples to be measured are shown in Figure 8.

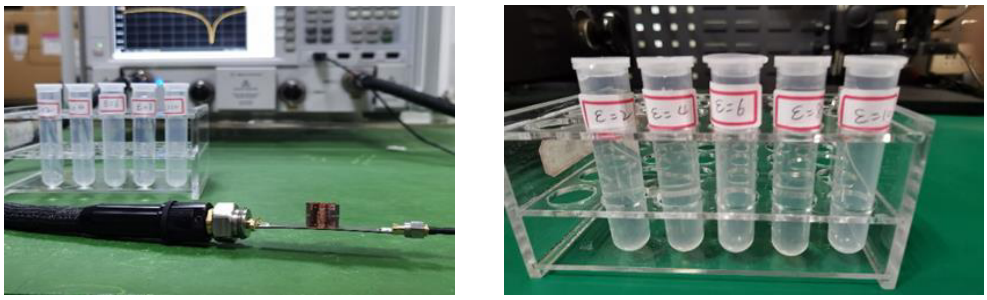

Figure 8. Test platform building. (a) Experimental environment; (b) samples to be measured.

To avoid corrosion of the sensor, a new plastic film is added to the inner wall of the container during each test. Five groups of 2 ml LUTs were put into containers for S_{11} parameter measurement. Figure 9 and Table 2 show the comparison of measured and simulated results.

It can be seen from Table 2 that when the designed sensor is used to test the dielectric constant of the object to be measured, the error of the real part is controlled within 2%, and the accuracy is high. According to the definition of sensitivity [18]:

$$s = \frac{\Delta f[\%]}{\Delta \varepsilon_r} = \frac{f_2 - f_1}{f_1(\varepsilon_2 - \varepsilon_1)}$$

Table 2. Comparison of measurement results.

No.	1	2	3	4	5	6
ε_r (Reference)	1.00	2.00	4.00	6.00	8.00	10.00
ε_r (Measured)	1.08	2.07	4.79	6.61	8.06	10.04
Relative error %	0.10	2.0	0.22	0.16	0.75	0.10

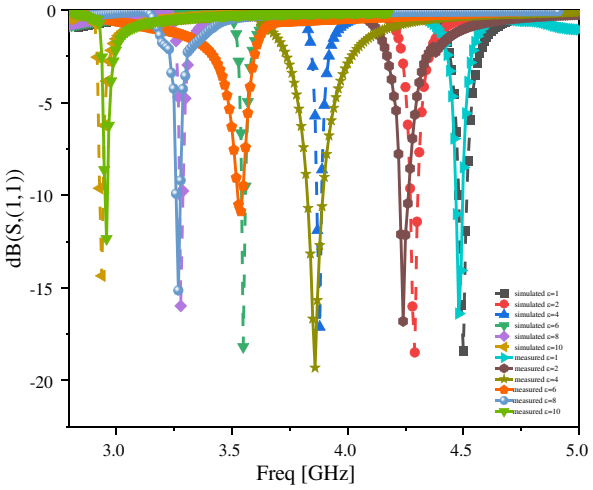

Figure 9. Measured and simulation results of S_{11}.

According to the measurement results, the sensitivity of the sensor is up to 3.85%. Based on the analysis of the existing errors, we have obtained the following reasons. The errors introduced during welding of SAM joints mainly come from the fabricating errors of plates and some inevitable factors in the process of processing and testing.

Table 3 shows the comparison between this work and other proposed sensors. It can be concluded that the designed sensor has the advantages of high sensitivity.

Table 3. Comparison between the proposed and referenced sensors.

Ref.	Main Structure	Sensitivity (%)	Type
[11]	SIW	0.27%	container
[14]	SIW-CSRR	2.20%	intrusive
[19]	CSRR	1.00%	container
[20]	SIW-CSRR	3.04%	intrusive
This work	SIW-CSRR	3.85%	container

5. CONCLUSIONS

In this work, a microwave sensor for measuring the dielectric constant of liquid is proposed. To solve the problem that the electric field of the container sensor only exists in the plane substrate, this work uses the structural characteristics of flexible materials to transfer the electric field from the plane substrate to the inner wall of the container.

The flexible dielectric substrate loaded with SIW-CSRR enhances the electric field distribution during liquid detection and improves the sensitivity of the sensor. The experimental result shows that

the sensitivity of the sensor reaches 3.85%. Compared with other sensors of the same type, the sensor combines the resonance characteristics of CSRR and the structural advantages of SIW, showing the characteristics of high measurement accuracy and high sensitivity. This work provides a reference for the design and application of high sensitivity measuring the dielectric constant of liquid in the future.

REFERENCES

1. Mohamed, A., R. Amar, and H. Cherif, "Hyper-sensitive microwave sensor based on split ring resonator (SRR) for glucose measurement in water," *Sensors and Actuators A: Physical*, Vol. 321, 0924–4247, Apr. 2021.
2. Marathe, D. and K. Kulat, "A compact dual, triple band resonators for negative permittivity metamaterial," *AEU-International Journal of Electronics and Communications*, Vol. 88, 157–165, May 2018.
3. Ilona, P., W. Krzysztof, and G. Slawomir, "Detection of methanol contamination in ethyl alcohol employing a purpose-designed high-sensitivity microwave sensor," *Measurement*, Vol. 174, 0263–2241, Apr. 2021.
4. Hamed, R., M. Maani, and J. Babak, "Towards a machine-learning-assisted dielectric sensing platform for point-of-care wound monitoring," *IEEE Sensors Letters*, Vol. 4, No. 6, 1–4, Jun. 2020.
5. Viktorija, M., J. Aaron, and J. Simon, "Passive wireless UHF RFID antenna label for sensing dielectric properties of aqueous and organic liquids," *IEEE Sensors Journal*, Vol. 19, No. 11, 4299–4307, Jun. 2019.
6. Li, L., H. Hu, P. Tang, B. Chen, J. Tian, and S. Safavi-Naeini, "A modified open-ended rectangular waveguide based reflection approach for dielectric constant characterization of low-loss slab materials," *IEEE Transaction Antennas and Propagation*, Vol. 69, No. 11, 8009–8014, May 2021.
7. Rasidian, A., L. Shafai, D. Klymyshyn, and C. Shafai, "A fast and efficient free-space dielectric measurement technique at mm-wave frequencies," *IEEE Antennas and Wireless Propagation Letters*, Vol. 16, 2630–2633, Aug. 2017.
8. Peng, Z., J. Hwang, and M. Andriese, "Maximum sample volume for permittivity measurements by cavity perturbation technique," *IEEE Transactions on Instrumentation and Measurement*, Vol. 63, No. 2, 450–455, Feb. 2014.
9. Koirala, G., R. Dhakal, and E. Kim, "Radio frequency detection and characterization of water-ethanol liquid through spiral-coupled passive micro-resonator sensor," *Sensors*, Vol. 18, No. 4, Apr. 2018.
10. Amir, E., W. Withawat, and A. Said, "High-sensitivity metamaterial-inspired sensor for microfluidic dielectric characterization," *IEEE Sensors Journal*, Vol. 14, No. 5, 1345–1351, May 2014.
11. Abdolrazzaghi, M., D. Mojgan, and K. Ashwin, "Strongly enhanced sensitivity in planar microwave sensors based on metamaterial coupling," *IEEE Transactions on Microwave Theory and Techniques*, Vol. 66, No. 4, 1843–1855, Apr. 2018.
12. Sadat, J. F. and A. S. Javad, "Reconfigurable microwave SIW sensor based on PBG structure for high accuracy permittivity characterization of industrial liquids," *Sensors & Actuators A Physical*, Vol. 283, 386–395, Jun. 2018.
13. Nilesh, K., P. Surya, and A. Jaleel, "Novel improved sensitivity planar microwave probe for adulteration detection in edible oils," *IEEE Microwave and Wireless Components Letters*, Vol. 29, No. 2, 164–166, Feb. 2019.
14. Reyes-Vera, E., G. Acevedo-Osorio, M. Arias-Correa, and D. E. Senior, "A submersible printed sensor based on a monopole-coupled split ring resonator for permittivity characterization," *Sensors*, Vol. 19, No. 8, 1936–1936. Apr. 2019.
15. Arani, A. and K. Mrinal, "Miniaturized substrate integrated waveguide (SIW) power dividers," *IEEE Microwave and Wireless Components Letters*, Vol. 26, No. 11, 888–890, Nov. 2016.

16. Feng, X. and K. Wu, "Guided-wave and leakage characteristics of substrate integrated waveguide," *IEEE Transactions on Microwave Theory and Techniques*, Vol. 53, No. 1, 66–73, Jan. 2005.
17. Salim, A. and S. Lim, "Complementary split-ring resonator-loaded microfluidic ethanol chemical sensor," *Sensors*, Vol. 16, No. 11, 1802–1802, Nov. 2016.
18. Humberto, L., C. Alonso, L. José, A. Ricardo, P. Chávez, and L. José, "Wireless sensing of complex dielectric permittivity of liquids based on the RFID," *IEEE Transactions on Microwave Theory and Techniques*, Vol. 62, No. 9, 2160–2167, Sep. 2014.
19. Sadat, J. F. and A. S. Javad, "Reconfigurable microwave SIW sensor based on PBG structure for high accuracy permittivity characterization of industrial liquids," *Sensors & Actuators A Physical*, Vol. 283, 386–395, Jun. 2018.
20. Galindo, R., M. Herraiz, and V. Segovia, "Submersible printed split-ring resonator-based sensor for thin-film detection and permittivity characterization," *IEEE Sensor Journal*, Vol. 16, No. 10, 3587–3596, May 2016.